Rolling GPS Receiver Development and Verification Testing for Space Application

David Yale, *Stanford University*
Awele Ndili, *Stanford University*
Jie Li, *Stanford University*
Ellen Ng, *Lockheed Martin Missiles and Space*
Eric Bean, *Stanford University*
Saps Buchman, *Stanford University*

BIOGRAPHY

David Yale, works with Gravity Probe B Science Mission team, and has been involved in the development and testing of the GPS receiver to be used on the GP-B spacecraft. He received his B.S. degree from San Francisco State University.

Awele Ndili, Ph.D., is the project manager for GPS receiver development for the Gravity Probe B Relativity Mission at Stanford University. He received his Ph.D. and M.S. degrees from Stanford University. He has been working on GPS systems since 1992.

Jie Li, Ph.D., is a visiting scholar in the Gravity Probe B Relativity Mission at Stanford University. He received his Ph.D. degree from the Chinese Academy of Space Technology in Beijing, P. R. China.

Ellen Ng, works with Gravity Probe B Science Mission team, and has been involved in software development and testing of the GPS receiver to be used on the GP-B spacecraft.

Eric Bean is a research assistant involved in the testing of the GPS receiver to be used on the GP-B spacecraft. He received his B.S. degree in aerospace engineering from the University of Virginia.

Saps Buchman, Ph.D., is the hardware manager for the Gravity Probe B Relativity Mission at Stanford University. He received his Ph.D. degree in physics from Harvard University.

ABSTRACT

This paper presents results of GPS receiver development and verification tests with a rolling space vehicle simulator for the Stanford Gravity Probe B (GP-B) Relativity Mission. The GP-B spacecraft will carry two redundant units of Trimble's TANS Vector GPS receiver to provide real-time navigation solutions for orbit trim, raw GPS measurements for ground processing which will be used to generate more accurate position and velocity for science data calibration, and the Pulse-Per-Second (PPS) timing signal to payloads. During its science mission in a circular, polar orbit at the 650km height, the GP-B spacecraft will roll in an inertially fixed direction of a guide star. The roll rate will be between 0.1 rpm and 1.0 rpm. The antenna selection algorithm will determine the visibility of GPS satellites and assign a master antenna to each of six receiver channels to maintain continuity of the signal tracking. A rolling spacecraft simulator is developed for the verification tests of the GPS receiver. Four antennas are configured as they will be on the GP-B spacecraft on a horizontal axis with the GPS receiver. A variable speed DC motor mechanically coupled to the axis 'rolls' the GPS antennas and receiver at up to two times the anticipated roll rate of GP-B, providing real signals for software development and testing. Data of experiments with the rolling spacecraft simulator are presented in this paper, and the special points related to the roll of the spacecraft are emphasized. Some data processing techniques with a monitor named "Solution-Quality-Indicator" (SQI) are also introduced, which improves the real time performance of navigation solutions.

INTRODUCTION

The primary objective of the Gravity Probe B (GP-B) program is to measure the relativistic drift of an Earth-orbiting gyroscope as predicted by Einstein's theory of General Relativity [1]. The GP-B spacecraft will carry two redundant units of Trimble's TANS Vector GPS receiver to provide real-time navigation solutions for orbit trim, raw GPS measurements for ground processing which will be used to generate more accurate position and velocity for science data calibration, and the Pulse-Per-Second (PPS) timing signal to payloads [2, 3].

During its science mission in a circular, polar orbit at the 650km height, the GP-B spacecraft will roll in an inertially fixed direction of a guide star. The roll rate will be between 0.1 rpm and 1.0 rpm. The four antennas of the GPS receiver are aligned in different directions, resulting in a complete field of view so that continuous visibility of GPS satellites will be maintained while the GP-B spacecraft rolls. Fig.1 illustrates the GP-B spacecraft and the GPS antenna configuration.

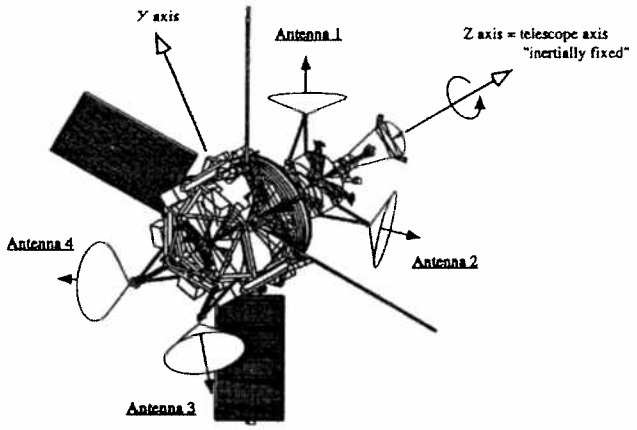

Fig.1 GP-B spacecraft and GPS antenna configuration

The TANS Vector GPS receiver can track up to six GPS satellites, one on each channel. Each channel's varying "master" antenna provides the signal used for code and carrier tracking, while the other three antennas provide differential phase measurements, referenced to the master antenna. The designation of master antenna can vary from channel to channel, and it can also vary from time to time for each channel.

The GPS receiver satellite/antenna selection algorithm will determine the visibility of GPS satellites and assign a satellite and a master antenna to each receiver channel in order to maintain signal tracking. Based on the antenna Field-Of-View (FOV) analysis, it will be shown that the GPS satellite selection algorithm and the antenna selection algorithm can be de-coupled. A previous paper [4] discussed the GPS satellite selection problem, and presented a four-step selection algorithm, which showed good performance of both the navigation accuracy and the continuity of signal tracking. This paper will focus on the antenna selection algorithm and the related verification testing.

A rolling spacecraft simulator, developed by NavAstro and Gravity Probe B, is used in the verification tests of the GPS receiver. Four antennas are configured similar to the configuration on the GP-B spacecraft on a horizontal axis with the GPS receiver. A variable speed DC motor mechanically coupled to the axis 'rolls' the GPS antennas and receiver at up to two times the anticipated roll rate of GP-B, providing real signals for software development and testing.

Data of experiments with the rolling spacecraft simulator are presented in this paper, and the special points related to the roll of the spacecraft are emphasized. Considering some abnormal modes of the receiver and the related spikes in the navigation solutions, a monitor named as "Solution-Quality-Indicator" (SQI) is introduced, which captures integrity information between the update period of the receiver and provides a robust and versatile parameter for the data filtering. The data both before and after the processing with SQI are shown in the paper, demonstrating the effectiveness of the SQI.

This paper is organized as follows: First, the field-of-view (FOV) of antennas is analyzed and the antenna selection algorithm is described. Then the design of the rolling spacecraft simulator is given and the experiment data are presented. Considering some problems in the output data, the concept of the SQI is introduced, and some data filtered with SQI are also presented for the performance comparison. Finally, conclusions are derived.

ANTENNA FIELD-OF-VIEW ANALYSIS

As illustrated in Fig.1, GP-B has a science telescope pointed at the guide star. Four antennas of the GPS receiver are aligned in different directions: The forward antennas 1 and 2 are 45° apart from the bore-sight axis of the telescope, and the aft antennas 3 and 4 are 135° apart from it. Antennas 1 and 2 are perpendicular to one another and out of phase by 180°, and so are antennas 3 and 4. The aft set is out of phase by 90° from the forward set.

Define a body-centered body-fixed coordinate system: O_B is at the mass center of GP-B, $\vec{Z}_B$ is aligned in the bore-sight axis of the science telescope, $\vec{X}_B$ and $\vec{Y}_B$ are fixed to the body of GP-B and complete the right-handed triad. The nominal azimuth angles and elevation angles (referenced to the plane $O_B - \vec{X}_B\vec{Y}_B$) of the four antennas are given in Table 1.

	Azimuth angle	Elevation angle
Antenna 1	90°	45°
Antenna 2	270°	45°
Antenna 3	0°	-45°
Antenna 4	180°	-45°

Table 1. Azimuth and elevation angles of antennas

Fig.2 shows the combined Field-Of-View (FOV) of four antennas in $O_B - \vec{X}_B\vec{Y}_B\vec{Z}_B$. The solid lines denote the

edges of the FOV for each antenna. Since the FOV's for the antennas overlap, the numbers in each area denote which antennas share that portion of the view. It is also shown that the FOV's of antennas 1 and 2 are obstructed by the sunshade of the telescope.

It is clear that the combined FOV of the four antennas covers the entire sky with a solid angle of 4π steradian. Any GPS satellite visible to GP-B is located in the FOV of at least 1 antenna, and at most 3. Thus, the GPS satellite selection algorithm and the antenna selection algorithm can be de-coupled. In this paper the antenna selection algorithm and the related verification testing will be discussed.

While GP-B rolls in the direction of the guide star, the FOV of the antennas will also rotate in the inertial space. For a specific GPS satellite being tracked, it goes through the FOV's of several antennas, so that the master antenna has to be transferred among the antennas to keep the continuity of the signal tracking.

Let us consider the trace of a GPS satellite in the body-centered body-fixed coordinate system $O_B - \vec{X}_B\vec{Y}_B\vec{Z}_B$. Since the roll period of GP-B is very short compared to the orbital period of GPS satellites, the direction vector of a GPS satellite remains effectively fixed in inertial space during one roll period. It traces out a cone in $O_B - \vec{X}_B\vec{Y}_B\vec{Z}_B$, and the body elevation angle (the angle referenced to the plane $O_B - \vec{X}_B\vec{Y}_B$, positive in the direction of $\vec{Z}_B$) remains constant. Fig.2 shows that the direction vectors with a body elevation angle of 75° to 90° remain in the FOV of antennas 1 and 2 during an entire roll period, while those with an angle of -90° to -65° remain in the FOV of both antennas 3 and 4: in each case, no antenna transfer is necessary. The direction vectors with the body elevation angle of 30° to 75° and -65° to -30° must be transferred between antennas 1-2 and 3-4 respectively, while those with angles of -30° to 30° must be transferred among antennas 1-2-3, 1-2-4, 1-3-4, or 2-3-4. In addition, the transfer between two antennas should be done in the common FOV to prevent tracking discontinuities.

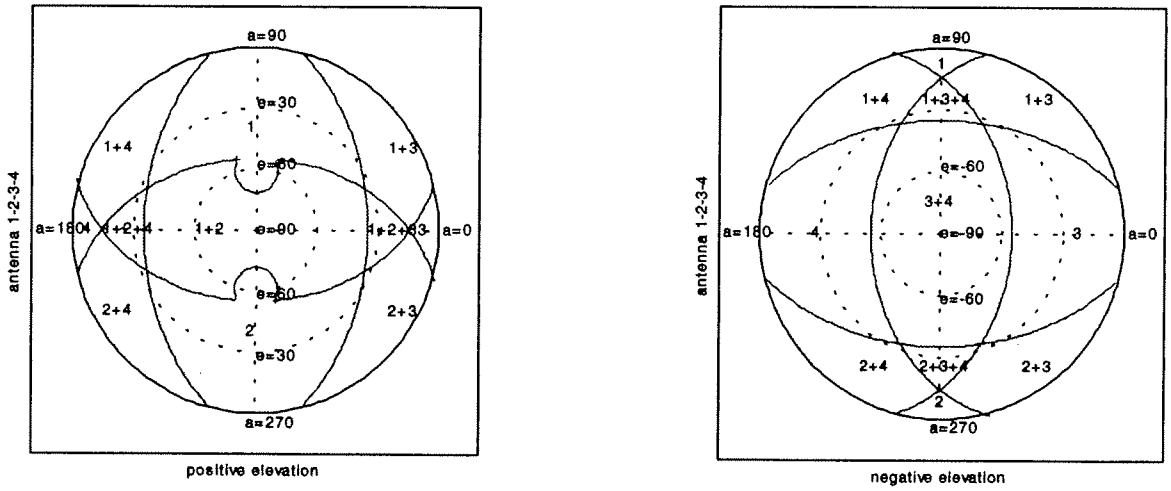

Fig.2 Combined field-of-view of four antennas

ANTENNA SELECTION ALGORITHM

The antenna selection algorithm will ascertain the visibility of GPS satellites and assign a master antenna to each of the six receiver channels in order to maintain continuity of the signal tracking.

Considering the available information for the GPS receiver onboard the GP-B spacecraft, there are two choices for the master antenna selection:

(1) The receiver has measurements of the Signal-to-Noise-Ratio (SNR) in each of the four antennas, so that the master antenna can be assigned to the antenna with the largest SNR.

(2) The attitude parameters of the GP-B spacecraft (available from the attitude control subsystem) can be used to determine the direction vectors of GPS satellites in the body-centered body-fixed coordinate system $O_B - \vec{X}_B\vec{Y}_B\vec{Z}_B$. Therefore, the antenna in which the GPS satellite has the highest elevation

angle with respect to that antenna's ground plane can be assigned as the master antenna.

The first algorithm is autonomous, i.e., it is independent of an external information source and is more robust in case of internal spacecraft communication failure. Hence it is chosen as the baseline antenna selection algorithm and is discussed in more detail below.

The SNR of the GPS signal in an antenna is mainly a function of that satellite's elevation angle referenced to the antenna's ground plane (antenna elevation angle). As illustrated in Fig.3, the SNR is large when the antenna elevation angle is large and small when the antenna elevation angle is small. When the antenna elevation angle is below a specific value (the mask angle), the SNR will be below the reception threshold, and no signal will be tracked.

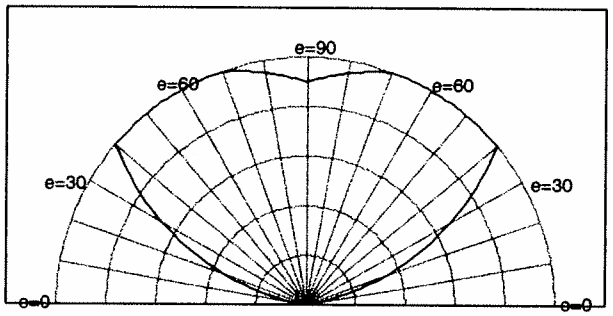

Fig.3 SNR vs. the antenna elevation angle

The SNR measurement is used as an index for the master antenna selection, and the principle of the algorithm is to maximize the SNR of the master antenna. Fig.4 illustrates the master antenna selection procedure. Consider a GPS satellite being tracked by one of the receiver channels: its antenna elevation angles with respect to two antennas vary periodically while the GP-B spacecraft roll, as do the SNR measurements of the two antennas. The antenna selection algorithm compares the SNR measurements and assigns the master antenna to whichever antenna has the larger SNR. The master antenna transfer should occur at the point with equal SNR measurements of two antennas. However, several effects (SNR measurement noise, gain pattern variations from antenna to antenna, small measurement update rate to roll rate ratio, multi-path effects, etc.) act on the master antenna selection logic and lead to spurious switching and switching errors. Therefore, a hysteresis is introduced in the selection algorithm, i.e., the master antenna transfer will not occur until the SNR of the current master antenna is less than 80 percent of the SNR of the highest non-master antenna. The effect of the hysteresis is shown in Fig.4. (Notice the phase delay between the middle and bottom graphs.)

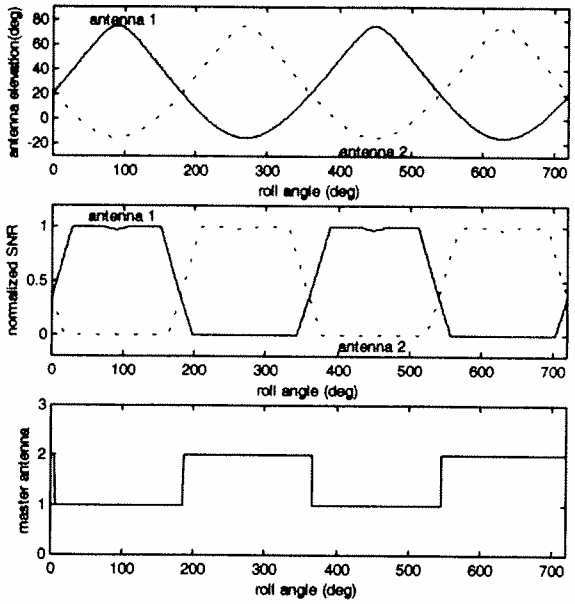

Fig.4 Procedure of the master antenna selection

ROLLING SPACECRAFT SIMULATOR

A rolling spacecraft simulator (Fig.5) was designed and fabricated to acquire live GPS signals for software development and verification testing.

The TANS Vector GPS receiver was mounted on the shaft axis. Four antennas were mounted in similar orientations as they will be on the GP-B satellite. The RF cables were routed inside the two-piece hollow shaft, allowing the shaft support bearings to be located inside the antenna support struts. This configuration shortened the overall physical dimensions allowing for better portability. Two shaft couplers and a slotted center section joined the two shaft halves and allowed the RF cables to exit the shaft interior near the TANS Vector mounting location.

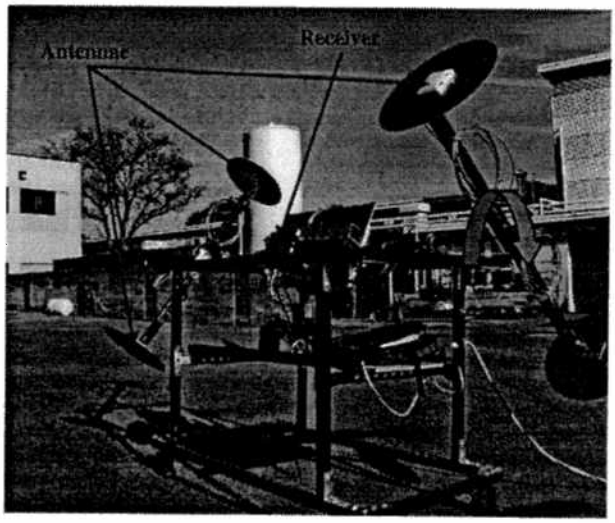

Fig. 5 Rolling spacecraft simulator

A 0-90 VDC, 0-9 rpm, variable speed, reversible gear motor mechanically powers the roll simulator through a 0.35" pitch drive chain and shaft mounted sprocket. Due to the torque characteristics of the motor, the simulator was found to not smoothly roll less than 0.4 rpm. Further speed reduction was necessary to acquire data at the lower limit of possible GP-B roll rates. Roll rates from 0.1 to 2.0 rpm were achieved by varying the voltage and gear/sprocket ratio.

Power and digitized data are conveyed across the stationary/rotating boundary by a 10 channel, 5 A / channel slip-ring, commercially purchased. A mid-shaft cross strut supports the stationary side of the slip ring as well as a terminal strip and a journal bearing located adjacent to the slip ring thus minimizing shaft eccentricity. The data cable to and from the slip-ring is RS-232 format, although RS-422 was found to work equally as well for our data transmission rates (19.2k baud).

One design consideration was portability: two people can easily disassemble and reassemble the roll simulator into three sections, allowing data acquisition at various locations such as an anechoic chamber at Lockheed Martin Missiles and Space, Sunnyvale (to approximate a space-like multi-path environment). The main location for data acquisition was on the HEPL rooftop, which offered minimal obstructions in visibility and thus minimized multi-path.

In an earlier design, the laptop was mounted on the shaft: A computer security device was used to mount the laptop, as well as batteries for the TANS Vector receiver power. This design was abandoned after problems developed in the laptop. Another support structure constructed out of welded steel proved to be disadvantageous during bearing alignment and thus was abandoned in favor of the modular and versatile Unistrut material.

DATA ANALYSIS

Data was acquired by first establishing the selected roll rate, then powering on the TANS Vector receiver. This sequence verified that the receiver will be able to acquire GPS satellites both initially (after the GP-B is rolling) and after an interruption in power to the receiver during flight. The receiver was able to acquire at all roll rates, up to our maximum tested rate of 2.0 rpm. Once acquisition started, we continued taking data at a constant roll-rate for approximately 2 hrs for each data set.

The master antenna assignment (see fig.6) is shown for channel 0 during a data set in which the SV# did not change for this channel. Packet count is along the horizontal axis, while master antenna number is on the vertical axis. Packet count is the sequential data packet identification number.

As mentioned earlier, the master antenna assignment occurs sequentially. For the upper graph, 0.18 rpm, the sequence is 3-2-1-0-3-2, etc. Ideally, the sequence of master antenna assignment would be identically repeated changing as a function of the GPS satellite orbit. As seen in figs 6 and 7, anomalies do occur, such as an out of sequence section of master antenna number: 3-2-1-0-3-0-3-0-3-2-1-0.

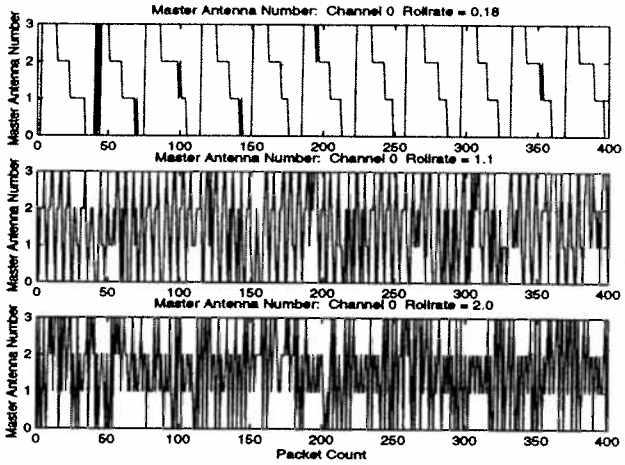

Fig.6 Master Antenna Number vs. Data Packet

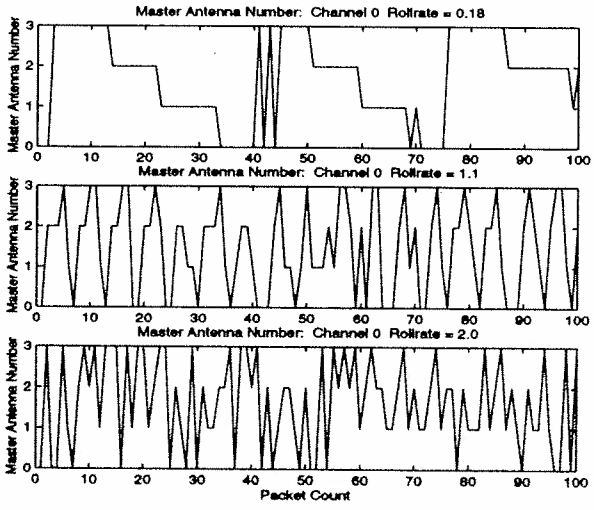

Fig. 7 Master Antenna Switching Zoom View

The master antenna selection mode employed compares the SNR for all four antennas every 15 sec. In higher rpm data sets, the master antenna selection algorithm SNR sampling might not occur when one particular antenna has the best visibility. Instead, the sampling occurs during the period when the following antenna has

the best visibility (and thus highest SNR), so that the master antenna assignment sequence skips the middle antenna, resulting in an out of sequence error, missing time periods of signal tracking and degraded receiver performance. This out-of-sequence error rate is a function of roll rate, with more out-of-sequence errors occurring in higher rpm data sets as in the middle and lower graphs, 1.1 rpm and 2.0 rpm respectfully.

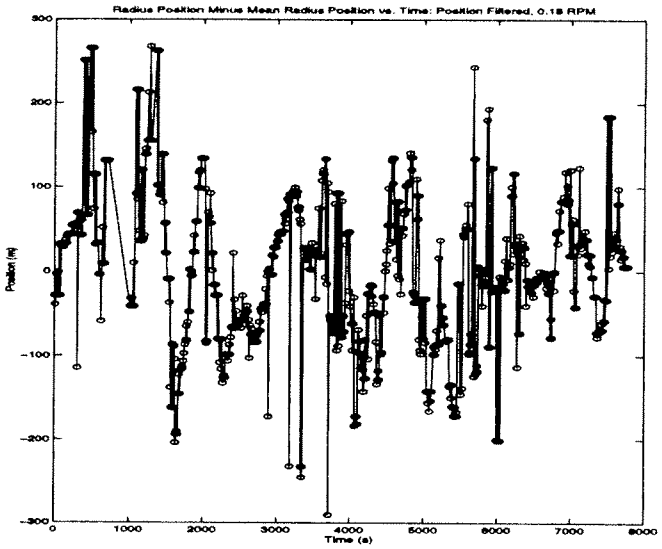

Fig. 8 R Position vs. Time for 0.18 rpm

Figure 8 shows R position data (where $R = (x^2 + y^2 + z^2)^{1/2}$, with respect to the known location) in meters versus time, acquired using the roll simulator at 0.18 rpm. The gross outlying data (|R – mean| > 300 m) have been filtered out. The standard deviation is 88.7 m.

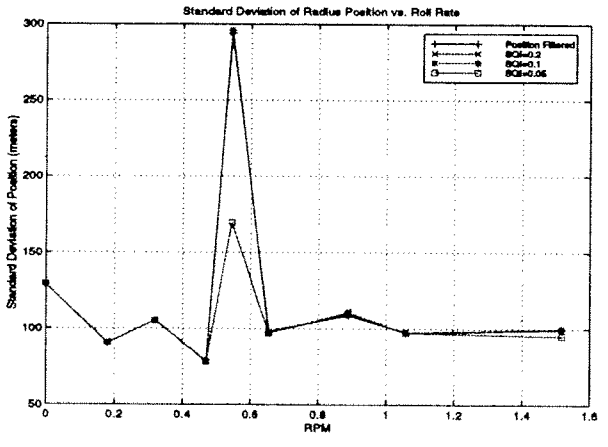

Fig. 9 Standard deviation of position vs. roll rate at various rpm

The standard deviations of position data for various roll rates are shown in fig. 9. There is a sharp transition at a roll rate between 1.5 and 2.0 rpm. This transition is most likely due to the original master antenna selection algorithm: at the higher roll rates, the receiver doesn't have a continuous high value SNR for each channel. Below 1.5 rpm, the variation can be attributed to inherent noise (e.g., selective availability, short data runs, etc.)

With various filter cuts, we will further reduce the standard deviations and eliminate most of the noise in the navigation solution data.

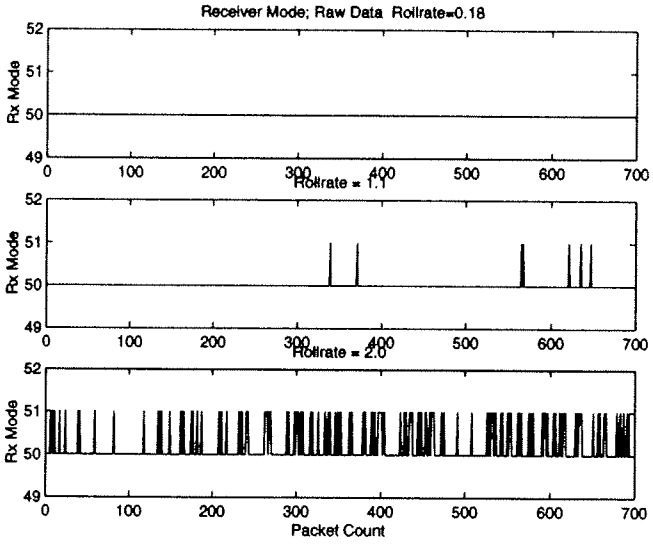

Fig. 10 Mode vs. Data Packet

RECEIVER MODE

Receiver mode is a measure of the integrity of the position and velocity solutions (Fig. 10). A value of 50 indicates normal position fixing mode, while a value of 51 indicates that there is a problem with the receiver integrity and thus the data is suspect. The receiver mode is a function of roll rate, with the higher roll rate data indicating a greater number of poor integrity data packets and lower reliability.

One explanation of the increasing number of mode 51 data packets with increasing roll rate is the master antenna selection algorithm. If the SNR sampling for comparison occurs at fixed time intervals greater than ¼ roll period, then the receiver will be utilizing the signal from an antenna which has a poor SNR for position fix, triggering a switch from mode 50 to mode 51.

Furthermore, although this data was acquired while rolling and with live GPS signals, the roll simulator was stationary during the data set. In practice, the GP-B satellite will be moving approximately 70 km between successive data points, which will introduce more error

into the navigation solution. So it is necessary for us to filter out the abnormal receiver mode 51 solutions as they will greatly increase the error in the navigation solution of the GP-B spacecraft.

SOLUTION QUALITY INDICATOR (SQI)

It is desirable to have a real-time parameter that can be used to make navigation solution data cuts in order to increase navigation accuracy and reliability without unduly affecting the solution availability. The receiver mode value is such a candidate for filtering as it indicates suspect data. However, due to spacecraft data flow control considerations, the receiver transmits navigation data packets (containing receiver mode information) at 1.0 Hz.

Between each successive data packet, the receiver is continuously tracking GPS satellites and generating all relevant solutions, including receiver mode (fig. 11). If the receiver switches to mode 51 between successive transmissions, the subsequent navigation solution accuracy is suspect.

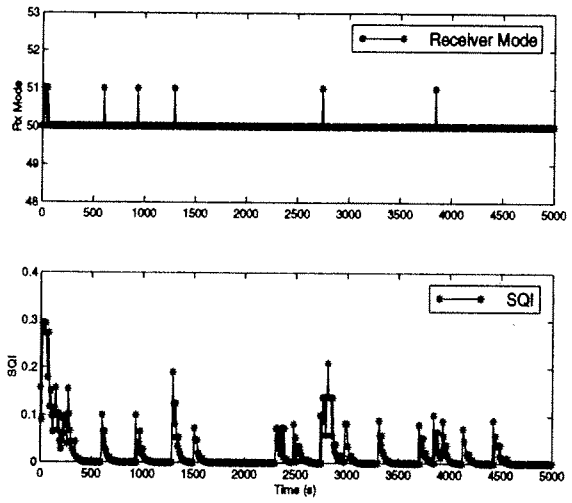

Fig. 11 Receiver Mode vs. Time and SQI vs. Time

The SQI parameter is a running average of the previous 10 solution's receiver mode, weighted more heavily towards the most recent receiver mode value. It ranges between 0 and 1, with 0 indicating that there hasn't been a mode 51 in the last 10 solution cycles (based on the receiver's intrinsic solution rate, not the data transmission rate). A value of 1 indicates that the previous 10 solutions were made while the receiver was in mode 51. Fig. 11 shows the variation in SQI during periods when the transmitted receiver mode had already returned to mode 50 (e.g., at time = 3400 s).

A robust and versatile parameter, SQI can be used to filter data by removing suspect data points that are near epochs when the receiver was in an abnormal mode.

DATA FILTERING

Our data filtering consists of first removing the gross position outliers. Next, we incorporate the SQI parameter, using various values of SQI to make data cuts by limiting the maximum value of SQI in the remaining data set.

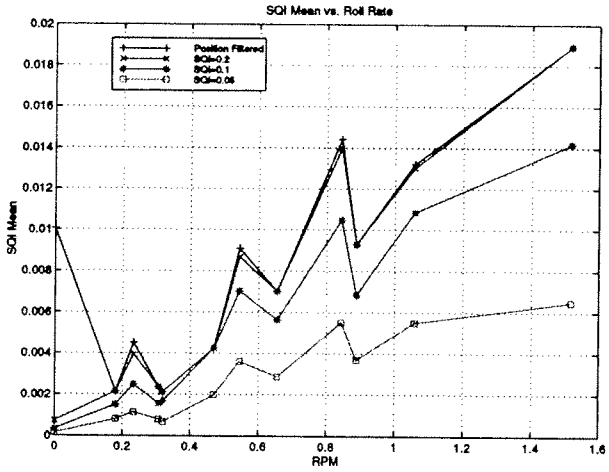

Fig 12 shows the mean of SQI at various roll rates, and reveals the dependence of that mean on roll rate. Thus, for a given SQI threshold, more data will be cut from a higher roll rate data set. Data filtering using SQI will have to take this effect into account and change the SQI threshold accordingly.

Fig. 12 SQI mean vs. roll rate

Ideally, we want to maintain the navigation solution availability as high as possible after filtering. Fig. 13 shows the availability of navigation solution data resulting from various SQI thresholds.

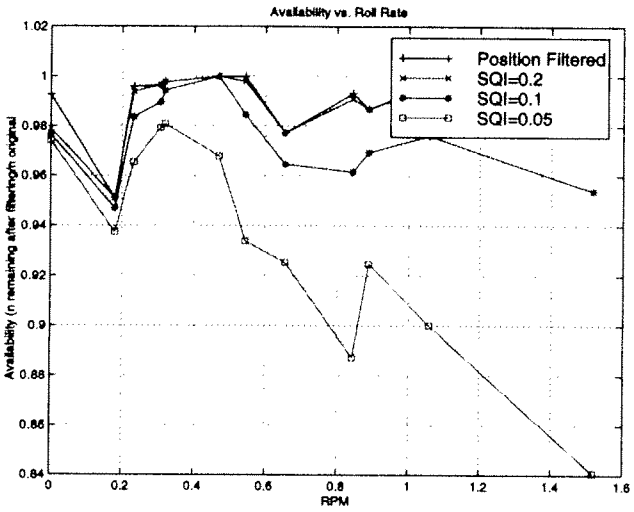

Fig. 13 Availability vs. roll rate

CONCLUSION

The roll simulator has provided a means to acquire live GPS data for GP-Bsoftware development and verification. The data shows that the TANS Vector receiver does acquire and track GPS signals while rolling at roll rates up to 2.0 RPM (maximum roll rate tested). The data also shows that performance degrades sharply above 1.5 RPM. Accuracy degrades from ... to ... . In addition, availability degrades from approximately 99% to ... SQI was implemented as a real-time and post-processing filter to maintain a high level of integrity. The SQI is very effective at RPMs greater than 1.0 RPM, however, there is a tradeoff between integrity and availability for a given accuracy. At roll rates under 1 RPM, the TANS vector receivier is shown to meet the GP-B required navigation performance of 100 m RMS 1-D and 1 m/s RMS.

ACKNOWLEDGEMENTS

Gratitude is acknowledged to NASA for supporting this research under Contract No. NAS8-39225. Trimble Navigation Ltd. Is gratefully acknowledged for its support. The authors would also like to thank Lockheed Martin Missiles and Space for the use of their facilities during testing. Thanks also go to Gerry Murphy of Design_Net Engineering for providing useful design information and to Doug Simpson for electronics support information.

REFERENCES

1. C.W.F.Everitt, "The Stanford Relativity Gyroscope Experiment(A): History and Overview", in *Near Zero: New Frontiers of Physics*, J.D.Fairbank, J.B.S.Deaver, C.W.F.Everitt, P.F.Michelson, Eds., W.H.Freeman and Company, New York, 1988, pp.587-639.

2. H.Uematsu, B.W.Pakinson and E.G.Lightsey, "GPS Receiver Design and Requirement Analysis for the Stanford Gravity Probe B Relativity Mission", *Proceedings of ION GPS-95*, The Institute of Navigation, Palm Springs, California, Sept. 12-15, 1995, pp.237-246.

3. H.Uematsu and B.W.Parkinson, "GPS Receiver Development and Verification Tests for Stanford Gravity Probe B Relativity Mission: Verification Test Plan and Preliminary Results", *Proceedings of ION GPS-96*, The Institute of Navigation, Kansas City, Missouri, Sept. 17-20, 1996, pp.1377-1385.

4. J. Li, A. Ndili, L. Ward, and S. Buchman, "GPS Receiver Satellite/Antenna Selection Algorithm for the Stanford Gravity Probe B Relativity Mission", *Proceedings of 1999 National Technical Meeting*, The Institute of Navigation, San Diego, California, Jan. 25-27, 1999, pp.541-550.